Search for central exclusive $\gamma\gamma$ production and observation of central exclusive e^+e^- production in pp collisions at $\sqrt{s} = 7$ TeV

Wenbo Li on behalf of the CMS Collaboration

School of Physics, and State Key Laboratory of Nuclear Physics & Technology, Peking University, Beijing, China

DOI: `http://dx.doi.org/10.3204/DESY-PROC-2012-02/343`

We present a search for central exclusive $\gamma\gamma$ production, $pp \to p + \gamma\gamma + p$, and the observation of central exclusive e^+e^- production, $pp \to p + e^+e^- + p$, in proton-proton collisions at $\sqrt{s} = 7$ TeV, for an integrated luminosity of 36 pb^{-1}. No diphoton candidate satisfies the selection criteria. An upper limit on the cross section for $E_T(\gamma) > 5.5$ GeV and $|\eta(\gamma)| < 2.5$ is set at 1.30 pb with 95% confidence level. Seventeen exclusive e^+e^- candidates are observed, along with an estimated background of 0.84 ± 0.28 (stat.) events, in agreement with the QED-based prediction of 16.5 ± 1.2 (syst.) events.

1 Introduction

In central exclusive production, $pp \to p + X + p$, the colliding protons emerge intact from the interaction, and all the energy transferred from the protons goes into a central color-singlet system. No other particles are produced aside from the central system, and large rapidity gaps are present. The three main types of exclusive processes are ascribed to $\gamma\gamma$ interactions (e.g. exclusive e^+e^- production), $\gamma\mathbb{P}$ fusion (e.g. exclusive Υ production) and $\mathbb{P}\mathbb{P}$ exchange (e.g. exclusive $\gamma\gamma$ or Higgs boson production), where $\mathbb{P}$ denotes a pomeron. This article presents a search for exclusive $\gamma\gamma$ production, and the observation of exclusive e^+e^- production in pp collisions at $\sqrt{s} = 7$ TeV [1]. The analysis is based on a data sample corresponding to an integrated luminosity of 36 pb^{-1} recorded in 2010 by the CMS experiment.

Exclusive $\gamma\gamma$ events can be produced via the $gg \to \gamma\gamma$ process through a quark loop, with an additional "screening" gluon exchanged to cancel the color of the interacting gluons, and so allow the protons to stay intact. The quantum chromodynamics (QCD) calculation of this diagram is difficult because the screening gluon has low squared-four-momentum-transfer Q^2, and extra soft interactions between the protons may produce particles that destroy the rapidity gaps — an effect quantified by the so-called rapidity-gap survival probability, which is poorly known theoretically. The study of exclusive $\gamma\gamma$ production may shed light on diffraction and the dynamics of pomeron exchange. In addition, exclusive $\gamma\gamma$ production provides an excellent test of the theoretical predictions for exclusive Higgs boson production.

Exclusive e^+e^- production is a quantum electrodynamics (QED) process, and the cross section is known with an accuracy better than 1%. Detailed theoretical studies have shown that in this case the corrections due to the rapidity-gap survival probability are well below 1%

and can be safely neglected [2]. Exclusive e^+e^- events provide an excellent control sample for other exclusive processes whose theoretical predictions are less certain, such as exclusive $\gamma\gamma$ production. Semi-exclusive e^+e^- production, involving single or double proton dissociation, is also considered as signal in this analysis. This process has larger theoretical uncertainties, and requires the knowledge of the rapidity-gap survival probability. In the rest of this article, exclusive events will be referred to as "el-el" events, while semi-exclusive events with either or both protons dissociated will be referred to as "inel-el" and "inel-inel" events, respectively.

The ExHuME event generator [3] is used to simulate exclusive diphoton events and to calculate their production cross section, which is an implementation of the perturbative calculation of the Durham KMR model [4]. The LPAIR event generator [5] is used to simulate both exclusive and semi-exclusive e^+e^- events. The rapidity-gap survival probability is not included in LPAIR. In order to simulate the fragmentation of the excited protons in the semi-exclusive case, the LUND shower routine implemented in the JETSET package [6] is used.

2 The CMS Detector

The central feature of the CMS apparatus is a superconducting solenoid, providing a field of 3.8 T. Within the field volume are the silicon pixel and strip tracker, the crystal electromagnetic calorimeter (ECAL) and the brass/scintillator hadron calorimeter (HCAL). The ECAL provides coverage in the pseudorapidity range $|\eta| < 1.479$ in the barrel region (EB) and $1.479 < |\eta| < 3.0$ in the two endcap regions (EE). The HCAL provides coverage for $|\eta| < 1.3$ in the barrel region (HB) and $1.3 < |\eta| < 3.0$ in the two endcap regions (HE). Muons are measured in gas-ionization detectors, which are made by using three technologies: Drift Tubes (DT), Cathode Strip Chambers (CSC), and Resistive Plate Chambers (RPC). In addition to the barrel and endcap detectors, the two hadronic forward calorimeters (HF) cover the region of $2.9 < |\eta| < 5.2$.

3 Event Selection

The selection of signal events proceeds in three steps. Exactly two photons or two electrons of opposite charge, each with $E_{\mathrm{T}} > 5.5$ GeV and $|\eta| < 2.5$, are required to be present in the triggered events. Photon or electron identification criteria are subsequently applied. Then, the events are required to satisfy the cosmic-ray rejection criteria. Finally, the exclusivity selection is performed in order to reject non-exclusive events as well as pileup events (events with any other inelastic pp interaction overlapping with the exclusive interaction).

Both exclusive diphoton and dielectron events were selected online by requiring the presence of two electromagnetic showers with a minimum E_{T} of 5 GeV. The first offline selection step is to require the presence of exactly two photon candidates or two electron candidates of opposite charge, each with $E_{\mathrm{T}} > 5.5$ GeV and $|\eta| < 2.5$, for the diphoton and dielectron analyses, respectively. These photon (electron) candidates are subsequently required to satisfy the identification criteria described in Ref. [1].

In order to remove cosmic-ray events, the two photons (electrons) are required to have timing consistent with that of particles originating from a collision. Furthermore, the two candidates are required to be separated by more than 2.5 rad in ϕ.

Exclusivity selection criteria are designed to select exclusive events by rejecting events having particles in the range $|\eta| < 5.2$ not associated with the two photon (electron) candidates. More specifically, it is required that there should be no additional tracks in the tracker, no additional

towers above noise thresholds in the calorimeters (EB, EE, HB, HE, and HF), and no track segments in the DTs and CSCs, where 'additional' means 'not associated to the two photons (electrons)'. The exclusivity selection efficiency for the used data sample is only 0.145, and is dominated by the losses due to the no-pileup requirement.

4 Results

No diphoton candidate survives the selection criteria. An upper limit on the production cross section is set employing a Bayesian approach at 95% confidence level:

$$\sigma^{E_T(\gamma)>5.5\text{ GeV},\,|\eta(\gamma)|<2.5}_{\text{exclusive and semi-exclusive }\gamma\gamma\text{ production}} < 1.30\text{ pb}$$

The upper limit is on the sum of the exclusive (el-el) and semi-exclusive (inel-el and inel-inel) $\gamma\gamma$ production cross sections, with no particles from the proton dissociation having $|\eta| < 5.2$ for the semi-exclusive case. A comparison between the present upper limit and four theoretical predictions (el-el only) is shown in Fig. 1. Two different PDF sets, MRST01 and MSTW08, from both leading-order and next-to-leading-order fits, are considered. The difference between leading-order and next-to-leading-order predictions reflects mostly the difference in the low-x gluon density ($\sigma \sim (xg)^4$ [8]). The upper limit measured in this analysis is an order of magnitude above the predicted cross sections with next-to-leading-order PDFs, while it provides some constraint on the predictions with leading-order PDFs. If the MSTW08-LO PDF is used, the probability of finding no candidate in the present data is less than 23%. The semi-exclusive $\gamma\gamma$ production cross section is much less known theoretically, but is expected to be of magnitude similar to that of the fully exclusive process [7].

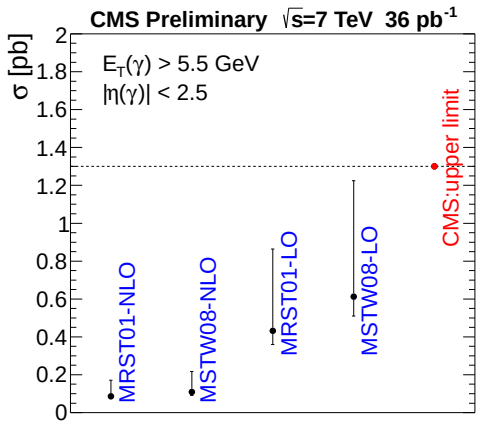

Figure 1: Comparison of the upper limit derived with the present data and four theoretical predictions (el-el only). If the contributions from semi-exclusive production are included, the predictions can increase by a factor of ∼2 [7].

Process	$\mathcal{L}$	σ	ε	Yield
el-el	$36.2 \pm 1.4\text{ pb}^{-1}$	3.74 pb	0.0488 ± 0.0056	6.57 ± 0.80 (syst.) events
inel-el		6.68 pb	0.0348 ± 0.0035	8.37 ± 0.90 (syst.) events
inel-inel		3.52 pb	0.0119 ± 0.0011	1.51 ± 0.15 (syst.) events
Total				16.5 ± 1.2 (syst.) events

Table 1: Predicted e^+e^- yields for both exclusive and semi-exclusive e^+e^- production. The integrated luminosity $\mathcal{L}$ has a relative uncertainty of 4% [9], and ε is the overall selection efficiency. The production cross sections σ are calculated with the LPAIR generator, and the poorly-known rapidity-gap survival probability is not included.

Seventeen exclusive e^+e^- candidates are observed with an expected background of 0.84 ± 0.28 (stat.) events, consistent with the theoretical prediction for the combined el-el, inel-el and inel-inel e^+e^- yields of 16.5 ± 1.2 (syst.) events (Table 1). Figure 2 shows the comparison of the

measured invariant-mass, p_{T} and $\Delta\phi$ distributions of the $\mathrm{e^+e^-}$ pairs with the MC simulation. Both the yield and the kinematic distributions are in good agreement with the assumption of exclusive $\mathrm{e^+e^-}$ production via the $\gamma\gamma \to \mathrm{e^+e^-}$ process, which validates the analysis technique, notably the exclusivity selection. The good agreement between the measurement and the simulation lends further support to the result of the exclusive $\gamma\gamma$ production search.

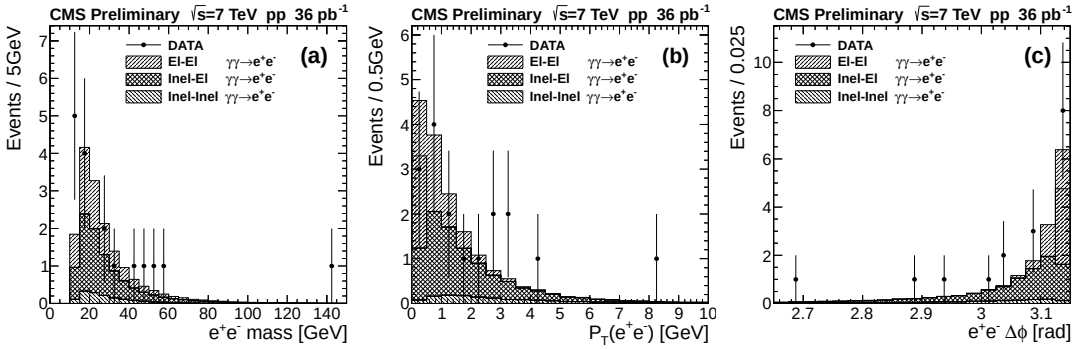

Figure 2: Distributions of the invariant mass (a), the transverse momentum (b), and the azimuthal angle difference (c) of the $\mathrm{e^+e^-}$ pairs, compared to the LPAIR predictions. The simulation is normalized to an integrated luminosity of 36 pb^{-1} and does not include the estimated 0.84 ± 0.28 background events.

5 Acknowledgements

The author would like to thank the National Natural Science Foundation of China and the China Scholarship Council for support.

References

[1] CMS Collaboration. CMS Physics Analysis Summary **FWD-11-004** (2012) . `http://cdsweb.cern.ch/record/1427001`.

[2] V. A. Khoze, A. D. Martin, M. G. Ryskin and R. Orava. Eur. Phys. J. **C19** (2001) 313–322, `arXiv:hep-ph/0010163`.

[3] J. Monk and A. Pilkington. Comput. Phys. Commun. **175** (2006) 232–239, `arXiv:hep-ph/0502077`.

[4] V. A. Khoze, A. D. Martin and M. G. Ryskin. Eur. Phys. J. **C23** (2002) 311–327, `arXiv:hep-ph/0111078`.

[5] S. P. Baranov et al. Physics at HERA, Proceedings of the Workshop (1991) 1478–1482.

[6] T. Sjostrand and M. Bengtsson. Comput. Phys. Commun. **43** (1987) 367–379. Especially Section 6.3: The Coherent Evolution Case.

[7] L. A. Harland-Lang, V. A. Khoze, M. G. Ryskin and W. J. Stirling. `arXiv:1204.4803`.

[8] L. A. Harland-Lang, V. A. Khoze, M. G. Ryskin and W. J. Stirling. Eur. Phys. J. **C69** (2010) 179–199, `arXiv:1005.0695`.

[9] CMS Collaboration. CMS Detector Performance Summary **DP-2011-002** (2011) . `http://cdsweb.cern.ch/record/1335668`.